

# Soil and climate affect foliar silicification patterns and silica-cellulose balance.

Félix de Tombeur<sup>1</sup>, Charles Vander Linden<sup>2</sup>, Jean-Thomas Cornélis<sup>1</sup>, Bruno Godin<sup>3</sup>, Philippe Compère<sup>4</sup>, and Bruno Delvaux<sup>2</sup>

<sup>1</sup>University of Liege

<sup>2</sup>Université catholique de Louvain

<sup>3</sup>Centre wallon de Recherches agronomiques

<sup>4</sup>Université de Liège

May 5, 2020

## Abstract

Silicon (Si) has beneficial effects in a variety of plant species and environments. Soil and climate affect silica accumulation in given plant species. Their roles on biosilicification patterns and balance between silica and C-rich biopolymers as structural components is poorly known. Here, we studied silica deposition in situ in sugarcane leaves collected in three tropical environments differing in soil and climate. Plant silica deposits were physically extracted from leaves through wet digestion. Leaves were observed and mapped for Si by ESEM-EDX. The C-rich biopolymers in leaves were determined by the Van Soest method. Silicon accumulation in leaf was related to bioavailable Si in soil and plant transpiration. Epidermal silica deposits were either limited to silica cells or expanded to long and short cells arranged in prominent veins fully silicified, depending on whether the leaf Si concentration was lowest or highest. The size of silica deposits increased with increasing leaf Si through an increasing number of conjoined silicified cells. Ash-free cellulose and Si concentrations were negatively correlated. Soil and climate impacted markedly the magnitude of biosilicification and the counterbalance between silica and cellulose as leaf structural components.

## Introduction

Since the recognition of the anomaly of silicon (Si) in plant biology (Epstein 1994), a number of advances have contributed to elevate Si to the status of beneficial substance. This recognition stimulates further progress towards the optimal exploitation of Si in agricultural practices. Si-induced functions in plant indeed alleviate various abiotic stresses (Adrees *et al.* 2015; Cooke & Leishman 2016; Meunier *et al.* 2017; Neu, Schaller & Dudel 2017), enhance plant protection against herbivores (McNaughton, Tarrants, McNaughton & Davis 1985; Keeping & Meyer 2006; Massey & Hartley 2006; Leroy, de Tombeur, Walgraffe, Cornélis & Verheggen 2019), pest and diseases (Fauteux, Rémus-Borel, Menzies & Bélanger 2005; Cai *et al.* 2008; Camargo, Amorim & Gomes Junior 2013) while they increase photosynthetic efficiency (Kang, Zhao & Zhu 2016) and plant biomass (Tubana, Babu & Datnoff 2016). Coskun *et al.* (2019) proposed a comprehensive model linking the Si-induced functions in plants through the “apoplastic obstruction hypothesis”. Their model defines Si as an “extracellular prophylactic agent against stresses (as opposed to an active cellular agent)”, and thus highlights the role of extracellular silica deposits on Si-induced functions.

Biosilicification in plant occurs in lumen and cell walls but also in extracellular and intercellular spaces (Yoshida, Onishi & Kitagishi 1959; Hodson, Sangster & Parry 1985; Kaufman, Dayanandan & Franklin 1985; Sangster, Hodson & Tubb 2001; Hodson 2019). Callose could be a “catalyst” for silica deposition (Law & Exley

2011; Exley 2015; Guerriero, Law, Stokes, Moore & Exley 2018). The structural role of silica in plants (Ando, Kakuda, Fujii, Suzuki & Ajiki 2002; Li *et al.* 2015) is attributed to the hardness property of silica (Perry & Fraser 1991; Perry & Keeling-Tucker 2000), which strengthens plant tissues (Epstein 1999; Bauer, Elbaum & Weiss 2011). Silica may indeed act as a compression-resistant structural component (Raven 1983; Epstein 1994), hence contributing to the mechanical resistance of vegetal structures. The inverse relationship between the concentrations of Si and of cellulose (Schoelynck *et al.* , 2010) or lignin (Bonilla, 2001; Klotzbücher *et al.* , 2017; Suzuki *et al.* , 2012; Yamamoto *et al.* , 2012) highlights the balance between Si and C components in plants (Cooke & Leishman 2012; Schaller, Brackhage & Dudel 2012; Schaller *et al.* 2019; Frew, Powell, Sallam, Allsopp & Johnson 2016; Simpson, Wade, Rees, Osborne & Hartley 2017). However, literature is lacking of evidence for the structural role of Si and thus balance with C-rich biopolymers (Bauer *et al.* 2011; Cooke, DeGabriel & Hartley 2016; Schoelynck & Struyf 2016; Soukup *et al.* 2017; Katz 2019).

Monosilicic acid ( $\text{H}_4\text{SiO}_4$ ) is taken up from soil solution, translocated to plant transpiration sites (Ma *et al.* 2006) where water loss promotes silica precipitation as amorphous opal-C ( $\text{SiO}_2 \cdot n\text{H}_2\text{O}$ ) forming phytoliths. The Si uptake in vascular plants depends on phylogenetic variation (Hodson, White, Mead & Broadley 2005; Deshmukh & Bélanger 2016), soil processes and properties (Lucas, Luizão, Chauvel, Rouiller & Nahon 1993; Meunier, Colin & Alarcon 1999; Henriët, Bodarwé, Dorel, Draye & Delvaux 2008a; Henriët, De Jaeger, Dorel, Opfergelt & Delvaux 2008b; Cornelis & Delvaux 2016; Quigley, Donati & Anderson 2016; de Tombeur, Turner, Laliberté, Lambers & Cornelis 2020), including soil physico-chemical and water properties (Li *et al.*, 2019; Rosen & Weiner, 1994; Quigley & Anderson, 2014), and climatic conditions (Jones & Handreck 1967; Euliss, Dorsey, Benke, Banks & Schwab 2005). An important soil property is the reserve of weatherable primary minerals, which represents the primary source of  $\text{H}_4\text{SiO}_4$  in soils, and thus of Si available for plants (Henriët *et al.* 2008a b; Klotzbücher *et al.* 2015).

Given the beneficial effect of foliar silicification on plant functions and stress regulation, understanding how environmental conditions impact this process is important. In addition, since a tradeoff between Si and C-rich biopolymers has been highlighted in literature, it deserves to be investigated under natural conditions, with a complete understanding of the factors controlling plant Si accumulation. Finally, an analysis of the biosilicification patterns could provide support for the mechanical role of silica and thus for the balance with C-rich biopolymers, which remains unclear in literature.

Here, we study the biosilicification patterns and balance between Si and C-rich biopolymers as leaf structural components in sugarcane cultivated in contrasting soil and climate conditions. We hypothesize that the reserve of soil weatherable minerals and evapotranspiration potential will be key drivers of the magnitude of silica deposits on leaf epidermis via contrasted level of Si accumulation. We further hypothesize that leaves with low foliar Si concentration will have higher cellulose concentrations as a mechanical compensatory role (Yamamoto *et al.* 2012; Guerriero, Hausman & Legay 2016).

## Materials and methods

### *Environmental setting*

Our fieldwork was carried out in sugarcane (*Saccharum officinarum* L.) exploitations established in three sites in Guadeloupe (16°15'N; 61°33'W). Soils largely differed (Table 1; Colmet-Daage & Lagache, 1965): they key out as Nitisol, Andosol and Vertisol in the WRB system (IUSS 2014). The Nitisol is highly weathered and formed from old andesitic ash (Colmet-Daage & Lagache 1965; Komorowski *et al.* 2005). The young Andosol (30–18 ka BP; Boudon *et al.* , 1987) developed on Eocene andesitic ash in perhumid conditions (Colmet-Daage & Lagache 1965). The Vertisol formed in smectitic materials derived from Pleistocene limestone (Komorowski *et al.* 2005) under drier conditions (Colmet-Daage & Lagache 1965). In the Nitisol-Andosol sites, MAP and MAT (Table 1, Fig. 1a) are, respectively 2910–3170 mm and 25.4–25.3°C whereas the mean relative ten-day ETP is 34.2–34.5 mm (Table 1). In the Vertisol site, MAP amounts to 1275 mm, MAT is 26.7°C whilst the mean relative ten-day ETP reaches 42.0 mm, and the average monthly precipitation is invariably below 100 mm from December to July (Fig. 1a). Monthly precipitation decreases from December to April in all sites. The wettest site is the Andosol one (Table 1) where the daily ETP measured during

the ‘dry’ season prior to fieldwork (Fig. 1b) shows very little variation in contrast to the Nitisol and Vertisol sites, in which a maximum value occurs in March. The water regime has greatly affected soil processes and mineral composition (Colmet-Daage & Lagache 1965). Abundant precipitation and intense leaching have enhanced mineral weathering and export of solutes to watersheds. The composition of the soils (Colmet-Daage & Lagache 1965) thus distinctly differs between the two wet sites and the Vertisol one, in agreement with the MAP threshold of 1400 mm above which humidity and intense leaching enhanced the processes of desilication and base exhaustion in similar environments, whilst below that threshold, silica and bases were retained (Chadwick *et al.* 2003). Soil processes have indeed led to the accumulation of secondary minerals such as kaolinite and Fe oxides in the Nitisol, Al-rich allophanic substances and gibbsite in the Andosol (Colmet-Daage & Lagache 1965; Ndayiragije & Delvaux 2003), denoting strong desilication (Churchman & Lowe 2012). In contrast, silica was retained in the Vertisol in which secondary Si-rich swelling clay minerals accumulate (Colmet-Daage & Lagache 1965). This mineralogical contrast originates from differences in soil age and soil moisture regime (Table 1), leading to decreasing water availability and increasing ETP in the sequence Andosol–Nitisol–Vertisol.

In these environments, sugarcane has long been cultivated. The sugarcane cultivars differed between sites (Table 1). *Saccharum officinarum* is a model Si-accumulator, but leaf Si concentration varies very little between cultivars ( $<0.02 \text{ g kg}^{-1}$ ) (Keeping *et al.*, 2013; Keeping & Meyer, 2006).

#### *Sample collection*

The topsoils were sampled at 0–20 cm soil depth in April 2017. The TVD (top visible dewlap) sugarcane leaves were sampled from primary shoots or stalks while tillers and suckers were avoided. The midrib was removed (McCray *et al.*, 2011). Topsoil and foliar samples were collected in triplicates in each site. For each replicate, three soil subsamples and twenty leaf subsamples were randomly collected to constitute a composite sample.

#### *Soil analysis*

Soil samples were air-dried and sieved at 2 mm. Soil pH was measured in  $\text{H}_2\text{O}$  and KCl 1 M with a solid:liquid ratio of 1g:5ml. Exchangeable cations and cation exchange capacity (CEC) were determined by 1 M ammonium acetate pH7 (Olsen, Sommers & Page 1982).  $\text{CaCl}_2$ -extractable Si ( $\text{CaCl}_2$ -Si) is considered to assess bioavailable Si in soils (Haymsom & Chapman 1975; Sauer, Saccone, Conley, Herrmann & Sommer 2006). Four grams of soil were shaken with 40 ml of a  $\text{CaCl}_2$  0.01 M solution for 6h. After centrifugation, the supernatant was filtered and analyzed for Si concentration by ICP-AES. Total elemental concentrations in soil were determined after calcination at 450 °C for 24 hours, followed by a fusion at 1000 °C for 5 min in a graphite crucible with Li-tetraborate and Li-metaborate (Chao & Sanzalone 1992). After dissolution of the fusion bead in 10%  $\text{HNO}_3$ , element concentrations were measured by ICP-AES. The total reserve in bases (TRB) in soils was computed as the sum of major alkaline and alkaline-earth cations (Ca, Mg, K and Na in  $\text{cmol}_c \text{ kg}^{-1}$ ) to estimate soil weathering stage (Herbillon 1986).

1. *Plant analyses*
2. *Si, Ca, Mg, K and C concentrations*

Leaf samples were thoroughly washed with 70% ethanol in order to remove potential particles from aeolian deposits. They were dried for four days in an oven at 65 °C and grinded. Si concentration was determined after calcination at 450 °C for 24 hours. The ash concentration was determined by weight difference before and after the calcination. Then, 100 mg of ashes were calcinated at 1000°C for 5 min in a graphite crucible with Li-tetraborate and Li-metaborate (Chao & Sanzalone 1992; Nakamura, Cornélis, de Tombeur, Nakagawa & Kitajima 2020). After the dissolution of the fusion bead in 10%  $\text{HNO}_3$ , the concentrations of Si, Ca, Mg and K were measured by ICP-AES. Carbon concentration in leaves was measured by flash dry combustion and expressed as dry weight (DW; 103 °C for 4 hours) and ash-free dry weight percentages respectively (AFDW).

#### *Fiber analysis*

Leaf fiber concentration was determined on grinded leaf samples according to the detergent fiber method

(Van Soest & Wine, 1967; Schoelynck *et al.* , 2010; Van Soest, 1973; Godin *et al.* , 2014, 2015). Briefly, on the one hand, the content of neutral detergent fibers (NDF containing cellulose, hemicelluloses and lignin) was determined using two extractants: (1) 0.1 mmol/L phosphate buffered at pH 7 for 15 min at 90°C, (2): Van Soest neutral detergent at 100°C for 1 h with the addition of sodium sulfite. The NDF fraction was incinerated at 550 °C for 3 h, and the mass loss allowed us to calculate the percentage of NDFom by difference (NDF without residual ash). On the other hand, the contents of acid detergent fibers (ADF containing cellulose and lignin) and acid detergent lignin (ADL containing lignin) were determined using the following extractants: (1) 0.1 mmol/L phosphate buffer at pH 7 for 15 min at 90°C, (2) Van Soest neutral detergent at 100°C for 1 h without the addition of sodium sulfite, (3) Van Soest acid detergent at 100°C for 1 h to get the ADF fraction, (4): sulfuric acid 72 % for 3 h to obtain the ADL fraction. The ADL fraction was incinerated at 550 °C for 3 h, and the mass loss allowed us to calculate the percentage of ADFom and ADLom by subtraction (ADF and ADL without residual ash). The cellulose, hemicellulose and lignin concentrations expressed as dry weight percentages (g kg<sup>-1</sup> DW) were then estimated as ADFom–ADLom, NDFom–ADFom, and ADLom, respectively (Godin *et al.* 2014, 2015). More details on the method can be found in Godin *et al.* , (2011). Finally, the three structural components were expressed as dry weight (g kg<sup>-1</sup> DW; 103 °C for 4 hours) and ash-free dry weight percentages (g kg<sup>-1</sup> AFDW).

#### *Physical extraction of silica deposits*

One of the three leaf samples from each site was used for physical extraction and microscopical observation of silica deposits. The extraction was carried out by wet digestion (adapted from Kelly, 1990; Frayse *et al.* , 2009; Corbinea *et al.* , 2013). Ten grams of washed and grinded leaf material were transferred into a glass baker with 10% HCl at 80°C to dissolve carbonates if any. Ultrapure 65% HNO<sub>3</sub> was gradually added in order to remove the major portion of organic tissues. Then, ultrapure the mixture 65% HNO<sub>3</sub>/30% H<sub>2</sub>O<sub>2</sub> was gradually added in the baker at 80°C as long as the reaction went on and the residue remained colorful. The residue was carefully rinsed with deionized water and transferred into polypropylene tubes for centrifugation at 3700 rpm for 5 min. Rinsing was repeated 3 times. The residue was oven dried at 50°C during 48h.

#### *SEM observation and X-ray microanalysis*

Extracted silica deposits were spread on glass slides covered with double-sided carbon tape and directly observed in a FEI ESEM Quanta 600 at 30 kV accelerating voltage and in low-vacuum mode (1.3 mbar).

Besides, leaf samples were mounted on glass slides using double-side carbon tape and bridged with silver paint before to carbon-coated in a Balzers MED010 evaporator. They were imaged with the backscattered-electron (BSE) detector in a FEI ESEM-FEG XL-30 working at 30 kV accelerating voltage and fitted with a Bruker 129 eV X-ray detector for elemental microanalysis. The Si distribution was obtained on the abaxial side of the leaves by elemental Si mappings acquired on the Si K $\alpha$  peak at 1.74 keV at 3 different magnifications (x38, x75 and x150). Stomata and dumbbell-shaped phytoliths per mm<sup>2</sup> of leaf surface were counted on the BSE images for the three magnifications, on five squares (200\*200 pixels, i.e. 0.41 mm<sup>2</sup>) randomly positioned on the images. In the same five squares, the area percentage of yellow pixels (Si signal) on Si elemental mappings was measured with the software GIMP v2.10.8.

#### *Statistical analyses*

Statistical analyses were performed using the software MiniTab®18.1. Means were compared based on least significant differences (LSD Fisher) and various letters were significantly different at the 95% level of confidence. Potential correlations were tested with Pearson's chi-square tests.

## **Results**

#### *Soil properties and mineral concentrations in plants*

As shown in Table 2a, soil pH was 5.8 (Nitisol, Andosol) and 7.2 (Vertisol) in water, 4.8 (Nitisol and Andosol) and 5.9 (Vertisol) in KCl. CEC (cmol<sub>c</sub> kg<sup>-1</sup>) was 25.8 in the Nitisol, 47.6 in the Andosol and 59.9 in the Vertisol. Base saturation in topsoils was 12% (Andosol) and 31% (Nitisol) in the wettest sites, but reached



85% in the Vertisol.  $\text{CaCl}_2\text{-Si}$  ( $\text{mg kg}^{-1}$ ) followed the sequence Nitisol (16.8) < Andosol (31.3) < Vertisol (55.1). TRB ( $\text{cmol}_c\text{kg}^{-1}$ ) followed the same trend (Table 2b): Nitisol (35) < Andosol (110) < Vertisol (114). Subtracting the exchangeable content from the total one for each cation gives the respective content of non-exchangeable base (Table 2b). Their sum represents the reserve of non-exchangeable bases, occluded in soil minerals. This reserve ( $\text{cmol}_c\text{ kg}^{-1}$ ) increases in the sequence: Nitisol (27) < Vertisol (63) < Andosol (104). Table 2b further shows that the content of non-exchangeable Mg largely contributed to the total non-exchangeable reserve.

#### *Mineral concentrations in plants*

The leaf Si concentration ( $\text{g kg}^{-1}$ ) (Table 3) followed the order Nitisol (7) < Andosol (14) < Vertisol (21). As far as the major cations are concerned, the sum of their contents ( $\text{cmol}_c\text{ kg}^{-1}$ ) followed the same sequence Nitisol (56) < Andosol (59) < Vertisol (79). The dominant cation in sugarcane leaves was K from the Andosol and Nitisol sites (>50%), but Ca from the Vertisol one (44%).

#### *Localization of leaf silica deposits*

As shown in Fig. 2, silica deposits can be classified into three different types according to their morphology and location: (i) surface dumbbell-shaped phytoliths located in silica cells (Fig. 2a), (ii) silicified guard cells of stomata arranged in rows (Fig. 2a) and (iii) silicified epidermal long and short cells arranged in longitudinal veins (Fig. 2b, c, d).

The size, forms and density (number per  $\text{mm}^2$ ) of the dumbbell-shaped phytoliths were constant whatever the site (Fig. 3a-j). Silica deposits in stomata were less important than in silica cells as evidenced by a lower yellow signal (Fig. 3g-i) and their density was significantly higher in leaves from the Andosol site as compared to the two other ones (Nitisol, Vertisol) (Fig. 3k).

The silicification in long and short cells greatly depended on the site as shown on Si mappings in Fig. 3. Indeed, the silicification in veins increased in the sequence Nitisol < Andosol < Vertisol. Prominent veins of about 20-70  $\mu\text{m}$  wide were formed by 2 to 3 rows of short broad epidermal cells (Fig. 3b-d), the lumens of which appeared fully silicified only at the Andosol and Vertisol site (Fig. 3e, f, h, i). Between these prominent veins, more flattened and wider veins (up to 200  $\mu\text{m}$ ) were located between longitudinal stomata rows and included several rows (5-10) of thin elongated epidermal cells. In the leaves from the Vertisol site, flat veins appeared strongly silicified compared to those from the Nitisol and Andosol site (Fig. 3a-i). Despite a high proportion of silicified stomata in the Andosol site, the total surface area affected by silicification significantly increased in the order Nitisol < Andosol < Vertisol (Fig. 3l).

#### *Structures of extracted silica deposits*

Extracted silica deposits showed different structures (Fig. 4): (i) silicified cell walls (Fig. 4a), (ii) silicified long cells (Fig. 4b) and short cells (Fig. 4c), (iii) elongated rod-shaped structures (Fig. 4d), (iv) silicified cell lumens (Fig. 4c, e), and (v) dumbbell-shaped phytoliths (Fig. 4f). Most of them corresponded to silica deposits occurring exclusively in epidermal cells. This is the case for dumbbell-shaped phytoliths and long and short silicified cells from veins. Other structures may correspond to silicified cells in inner tissues or to partial silicification. This is the case of silicified cell walls, cell lumens of different shapes and long rods. Deposits from stomata guard cells were not seen probably because of their small size and non-characteristic shape. Very large deposits up to 350  $\mu\text{m}$  long and 150  $\mu\text{m}$  wide and with several cells in thickness were observed (Fig. 4e).

The comparison of the 3 sets of 3 pictures in Fig. 5 taken at fixed magnification gives evidence that the size of silica deposits increased in the sequence Nitisol < Andosol < Vertisol (Fig. 5a-i). For the Nitisol site, small-sized dumbbell-shaped deposits (<50 $\mu\text{m}$ ) and short rod-spicules (most probably from stomata guard cells) dominated in leaves and multicellular deposits occurred only marginally (Fig. 5g). Large multicellular deposits up to 200  $\mu\text{m}$  were observed for the Andosol site (Fig. 5h), and even larger than 200  $\mu\text{m}$  for the Vertisol site (Fig. 5f, i).

### *Carbon, cellulose, hemicellulose and lignin concentration*

Ash concentrations ( $\text{g kg}^{-1}$  DW) significantly increased in the order Nitisol (54) < Andosol (66) < Vertisol (89) (Table 4). Carbon concentrations ( $\text{g kg}^{-1}$  DW) did not significantly differ between leaves from the wet sites Nitisol (469) and Andosol (465). They were significantly lower for the Vertisol site ( $455 \text{ g kg}^{-1}$ ). Leaf C and cellulose concentration was negatively correlated with Si concentration (Fig. 6a, c). After ash correction, C concentrations were similar for the three different sites (Fig. 6b), but cellulose concentrations ( $\text{g kg}^{-1}$  AFDW) significantly differed in the order Nitisol (374) > Andosol (365) > Vertisol (356) (Table 4) and was negatively correlated with Si concentration (Fig. 6d). After ash correction, the concentrations of hemicelluloses and lignin were not correlated to leaf Si concentration (Fig. 6e, f).

## **Discussion**

### *Control of soil and climate on leaf Si concentration*

The soil non-exchangeable reserve ( $\text{cmol}_\text{c} \text{kg}^{-1}$ ) of weatherable minerals (Table 2) is, by far, the largest in the Andosol (104): it is 3.8 and 1.6 times higher than in the Nitisol (27) and the Vertisol (63), respectively. In the Vertisol, total Ca massively includes exchangeable Ca, which accounts for 74% of total Ca, whereas exchangeable Mg represents only 16% of total Mg. In this soil, calcium carbonate provides exchangeable Ca, which contributes to saturate the exchange complex while non-exchangeable Mg is occluded in the octahedral sheet of smectite (Colmet-Daage & Lagache 1965). In this line, the Vertisol is very poor in primary silicate weatherable minerals, as confirmed by the near disappearance of feldspars (K) and Na-plagioclases (Table 2). Consequently, non-exchangeable Mg content is here the most pertinent indicator to discriminate the soil weathering stages between these three soils. Despite it directly impacts the leaf Mg concentration (Fig. 7a), non-exchangeable Mg content does not affect in the same way the leaf Si content (Fig. 7b), which is, by far, the largest in sugarcane leaves sampled in the Vertisol site, where it is controlled by bioavailable Si in soil (Fig. 7c). Thus, in the wet sites (Andosol, Nitisol), soil weathering stage primarily controls Si accumulation in sugarcane cropped in similar climate conditions as reported earlier for banana (Henriet *et al.* 2008a b) and rice (Klotzbücher *et al.* 2015). In contrast, in the Vertisol site, the impact of soil weathering stage is less important: climate affects water availability and plant transpiration (ETP, Table 1, Fig. 2) as well as smectite stability in soil, which is controlled by high silica activity in soil solution (Rai & Kittrick 1989) as promoted by the occurrence of a prolonged dry season (Colmet-Daage & Lagache 1965). In any case, the bioavailability of Si in soil here controls leaf Si content (Fig. 7c). Hypothesizing a negligible cultivar effect, our data thus corroborate that Si accumulation in a given plant species is affected by both the soil weathering stage (Henriet *et al.* 2008a b; Klotzbücher *et al.* 2015), and plant transpiration fluxes (Euliss *et al.* 2005; Henriet, Draye, Oppitz, Swennen & Delvaux 2006; Issaharou-Matchi *et al.* 2016).

### *Effect of environmental conditions on silicification patterns in sugarcane leaves*

Our data also highlight that soil and climate conditions affect biosilicification patterns in sugarcane leaves. As show in Fig. 3l, the relative area affected by silica deposits largely increases with the increase in  $\text{CaCl}_2$ -Si in soil and resulting leaf Si contents, from 13.5 % in Nitisol to 23.1% in Andosol and 38.7% in Vertisol sites. On the opposite, the number of dumbbell-shaped phytoliths are very similar between the three sites (Fig. 3j). Although a significant higher number of stomata per  $\text{mm}^2$  was observed for the Andosol site, the area affected by these silicified structures is small compared to the one of silicified veins. This is consistent with literature data showing that silica deposits in silica cells is an active and physiologically regulated process occurring during the first stage of leaf development, independently of transpiration rate (Motomura, Fujii & Suzuki 2004, 2006; Kumar, Milstein, Bami, Elbaum & Elbaum 2017a; Kumar & Elbaum 2018). In contrast, silica deposits in long and short cells is a passive process depending on silica saturation during cell dehydration (Kumar, Soukup & Elbaum 2017b; Alexandre *et al.* 2019). While the silicification of long and short cells depends on the leaf stage development (Alexandre *et al.* 2019), our results show that environmental conditions (soil, climate) also impact this process through Si plant-availability in soil (Hartley, Fitt, McLarnon & Wade 2015) and plant transpiration. Therefore, we suggest that environmental conditions have a direct influence on leaf epidermal silicification that directly controls some of the major Si-related functions as

defense against pathogen intrusion (Cai *et al.* 2008), herbivory (Epstein 2009; Keeping, Kvedaras & Bruton 2009) or water and UV stress (Meunier *et al.* 2017; Coskun *et al.* 2019).

It has been demonstrated that the leaf erectness of rice leaves was improved after Si fertilization (Yamamoto *et al.* 2012; Kido *et al.* 2015), the process being still debated (Bauer *et al.* 2011; Cooke *et al.* 2016). Our results show that the size of silica deposits extracted from the leaves increases with increasing leaf Si concentrations (Fig. 5). Larger Si bioavailability in soil and plant transpiration in the Vertisol site promote the formation of larger silica deposits, with more joint silicified cells. Here, we hypothesize that the formation of large multicellular silica deposits could be crucial to explain the increase in leaf erectness under Si fertilization. They are much larger, concern not only isolated epidermal cells but also deeper leaf tissues, and are thus probably more prone to play a mechanical role compared to deposits in silica cells and stomata of the epidermis. Indeed, they are especially concentrated in longitudinal reinforcement veins that thus could form continuous rigid silicified columns running all along leaf surfaces. Moreover, compact deposits of several cell columns not only concern epidermal cells but also involve deep plant tissues to form local rigid plates. This hypothesis should now be tested under controlled conditions, with a complete analysis of leaf mechanical properties.

#### *Balance between silica and cellulose as structural components*

Cellulose is majorly responsible for the biomechanical strength in plant leaves (Kitajima *et al.* 2012; Kitajima, Wright & Westbrook 2016). Since the deposition of silica is less energy-consuming than the biosynthesis of C-rich biopolymers (Raven 1983), tradeoffs may occur between these two types of structural components (Schoelynck *et al.* 2010; Klotzbücher *et al.* 2018; Schaller *et al.* 2019). Here, the ash-free C concentration does not differ between the 3 sites, highlighting the dilution of C by Si when no ash-corrections are made (Fig. 8) (Cooke & Leishman 2012). However, the leaf cellulose concentration ( $\text{g kg}^{-1}$  AFDW) decreases with increasing leaf Si concentration (Fig. 6d). This supports that cellulose is the C-rich biopolymer whose synthesis increases with decreasing silica deposits, a compensatory role for Si deprivation (Guerriero *et al.* 2016). The increase in cellulose synthesis in plants deprived in Si is located in the cell layer just beneath the abaxial epidermis and in short cells in the adaxial epidermis (Yamamoto *et al.* 2012), corresponding to the cell concerned with silica deposits in plants from Si-rich soils in this study (Fig. 4e). Therefore, the control of both the Si bioavailability in soil and plant transpiration on leaf Si concentration may modulate the synthesis of cellulose in epidermal cells, most probably those forming reinforcement veins, supporting the balance between C-rich biopolymers and silica reported earlier (Schoelynck *et al.* 2010; Suzuki *et al.* 2012; Klotzbücher *et al.* 2018).

#### *New insights on soil suppressiveness?*

Silicon-induced functions in plant enhance plant protection against a.o. fungal diseases (see e.g. (Fauteux *et al.* 2005; Fauteux, Chain, Belzile, Menzies & Bélanger 2006). On the other hand, in a given climatic context, Si bioavailability in soil largely depends on soil type and processes (Cornelis & Delvaux 2016). The spread of Panama disease, caused by *Fusarium oxysporum cubense* race 4 on banana, was governed by soil type as reported by Stotzky & Martin, (1963). These authors showed that this disease weakly developed in plants cropped on soils rich in swelling clays (smectite) whereas it led to the eradication of the sensitive banana cultivar *Gros Michel* in all other soils. This novelty was followed worldwide by a number of studies on various crops highlighting the presence of smectite as a factor suppressing plant diseases induced by soilborne pathogens (Stotzky 1986), leading to the concept of soil suppressiveness (Alabouvette 1999) and using soil clay mineral composition to predict this specific property (Stotzky 1986). The casual link between the occurrence of smectite and soil suppressiveness was, however, poorly established so far. Soil suppressiveness was proposed to be based on biotic interactions depending on abiotic characteristics of the soil, especially pH and the nature of clay minerals (Alabouvette 1999; Alabouvette, Olivain & Steinberg 2006). The impact of soil and climate conditions on Si accumulation in plant and biosilicification patterns reported here may open new routes in the appraisal of soil suppressiveness. Indeed, smectite is stable in soil at pH around or above neutrality and  $\text{H}_4\text{SiO}_4$  concentration over 1 mM in soil solution. Because of the plant protective Si-induced functions, the high bioavailability of Si in soil might thus contribute to the suppressiveness of high base

saturated swelling clayey soils, in addition to the effects of smectite properties on microbial ecology (Stotzky 1986; Alabouvette 1999). This challenging hypothesis requires, however, further investigation.

## Conclusion

Our data corroborate that soil weathering stage and plant transpiration strongly impact Si accumulation in plant. We further show that soil and climate affect the localization and size of silica deposits in leaves of sugarcane, a high-Si accumulator. These environmental factors thus play a crucial role on biosilicification patterns and likely on their resulting effects on the mechanical reinforcement of plant leaves and Si-related functions (Coskun *et al.* 2019). We further highlight that the increase in leaf Si concentration correlates with a lower synthesis of cellulose in sugarcane leaves. Yet, we cannot conclude on any casual mechanistic link between the increase in biosilicification magnitude and the decrease in cellulose concentration in sugarcane leaves. This should be further investigated since lignocellulosic and siliceous constituents do not play identical physiological roles in plants (Soukup *et al.* 2017).

## Acknowledgements

We express our gratitude to Dr. Marc Dorel and the staff of the CIRAD research station of Neuchâteau, Guadeloupe, for their assistance in field and laboratory work. We thank Briec Hardy and Alexis Durvieux for their field assistance, Anne Iserentant for her help in the UCLouvain soil laboratory, Richard Agneessens for the biochemical analysis in the CRA-W laboratory, and Meteo France for access to meteorological data. We are grateful to the Center for Applied Research and Education in Microscopy (CAREM) (ULiege) for providing access to electron microscopy. None of the authors declare conflicts of interest.

## Authors contribution

FdT, J-TC, BD and CVL planned and designed the research. FdT, CVL and BD conducted fieldwork. FdT, CVL, BG and PC performed experiments. FdT analysed data. All the authors wrote the manuscript.

## Figure legends

**Figure 1:** Monthly precipitation and temperature as averaged over 25 years (from 1993 to 2018) in the three sites (a). Daily ETP as measured from January to May 2017 in the selected sugarcane fields in (b). Leaf sampling took place from 11th to 13th April 2017 (green bars in b).

**Figure 2:** BSE-LV-SEM images performed on a sugarcane leaf (abaxial surface) from the Vertisol site (a-c) and combined image with EDX elemental mapping of Si (d). Intense white BSE (a-c) and yellow (d) signals indicate silica deposits. The horizontal and vertical arrows in (a) indicate, respectively, dumbbell-shaped phytoliths and stomata. The horizontal and vertical arrows in (b) and (c) indicate veins made of long cells and short cells, respectively.

**Figure 3:** Combined BSE-LV-SEM/EDX-Si mapping images of abaxial surfaces of sugarcane leaves from the three sites, at three direct magnifications (a-i). Number of dumbbell-shaped (DS) phytoliths per mm<sup>2</sup> (j) and stomata (k) for the three soils for MAG 1 and MAG 2. Relative area of yellow pixels (%) for the three soils and magnifications (l). The red square in (a) visualizes the area used for counting the number of phytoliths, stomata and yellow pixels.

**Figure 4:** BSE-LV-SEM images of extracted silica bodies from Vertisol sugarcane leaves. The arrow in image (b) indicates silicified long cells. The horizontal and vertical arrows in image (c) indicate respectively silicified short cells and cell lumens. The arrow in image (d) indicates a silicified rod-shaped structure. The horizontal arrow in image (e) indicate a large multicellular structure up to 350 µm long and 150 µm wide and the vertical arrow shows around 35 silicified cell lumens attached in length on this structure. The arrows in image (f) indicate dumbbell-shaped phytoliths.

**Figure 5:** Magnification series of BSE-LV-SEM views of silica structures extracted from leaves of sugarcane grown in the 3 different soils. Both particle size and number of large particles increase obviously from the Nitisol to the Vertisol. The arrows in images (f) and (i) indicate structures larger than 200 µm. The arrows

in image (g) show multicellular structures. The vertical, horizontal and diagonal arrows in image (h) indicate respectively attached cells lumens, long cells and short cells.

**Figure 6:** Plots of the carbon (a, b), cellulose (c, d), lignin (e) and hemicellulose (f) in  $\text{g kg}^{-1}$  DW (a, c) and  $\text{g kg}^{-1}$  AFDW (b, d, e, f) against Si concentration (in  $\text{g kg}^{-1}$  DW) in leaves from sugarcane cropped on the Nitisol (light brown), Andosol (orange-brown) and Vertisol (dark brown).

**Figure 7:** (a) Plot of sugarcane leaf Mg concentration against the content of non-exchangeable Mg in soil. (b) Sugarcane leaf Si concentration as plotted against soil  $\text{CaCl}_2$ -extractable Si content ( $\text{CaCl}_2$ -Si).

**Figure 8:** Plot of leaf ash concentration ( $\text{g kg}^{-1}$ ) against leaf Si concentration ( $\text{g kg}^{-1}$ ) in the *Poaceae* family ( $n=103$ ). Blue dots are the sugarcane leaves of this study. All the others are rice straw from Hasan *et al.*, 1993 in yellow, Shen *et al.*, 1998 in green, Abou-El-Enin *et al.*, 1999 in red and Agbagla-Dohnaniet *et al.*, 2001 in orange.

## Tables

**Table 1 :** Some general characteristics of the three sites and sugarcane cultivars.

Reference Soil Group <sup>1</sup>	Coordinates	Altitude m (asl)	Soil parent rock	MAP <sup>2</sup> mm	MAT <sup>3</sup> °C	ETP <sup>4</sup> mm/decade	Soil moisture regime <sup>5</sup>	Cultivar
Nitisol	16°10'36"N 61°38'04"W	163	andesitic ash (Pliocene)	2910	25.4	34.5	udic	R570
Andosol	16°02'59"N 61°35'33"W	150	andesitic ash (Eocene)	3170	25.3	34.2	perudic	R579
Vertisol	16°25'32"N 61°27'29"W	18	limestone (Pleistocene)	1272	26.7	42.0	ustic	B80689

<sup>1</sup> WRB key (IUSS 2014)

<sup>2</sup> Mean Annual Precipitation

<sup>3</sup> Mean Annual Temperature (2016, 2017)

<sup>4</sup> calculated from monthly and decade (10-day) data (2016, 2017)

<sup>5</sup> qualified following USDA's Soil Survey Laboratory Staff (2017), based on data from Colmet-Daage & Lagache (1965)

**Table 2 :** Selected soil properties: (a) Average ( $n=3$ ) values of pH, contents of exchangeable bases (Ca, Mg, K, Na), sum of exchangeable bases (SEB), cation exchange capacity (CEC), base saturation (BS),  $\text{CaCl}_2$ -extractable Si ( $\text{CaCl}_2$ -Si). For  $\text{CaCl}_2$ -Si, SE are given under brackets. (b) Average ( $n=3$ ) values of total elemental contents (Ca, Mg, K, Na), Total Reserve in Bases (TRB), contents of non-exchangeable bases (total – exchangeable content), total reserve of non-exchangeable bases.

Soil	pH	pH	Exchangeable bases ( $\text{cmol}_c$ $\text{kg}^{-1}$ )	Exchangeable bases ( $\text{cmol}_c$ $\text{kg}^{-1}$ )	Exchangeable bases ( $\text{cmol}_c$ $\text{kg}^{-1}$ )	Exchangeable bases ( $\text{cmol}_c$ $\text{kg}^{-1}$ )	SEB <sup>1</sup>	CEC	BS <sup>2</sup>	$\text{CaCl}_2$ - Si
	H <sub>2</sub> O	KCl	Ca	Mg	K	Na	$\text{cmol}_c$ $\text{kg}^{-1}$	$\text{cmol}_c$ $\text{kg}^{-1}$	%	mg $\text{kg}^{-1}$

Soil	pH	pH	Exchangeable bases (cmol <sub>c</sub> kg <sup>-1</sup> )	Exchangeable bases (cmol <sub>c</sub> kg <sup>-1</sup> )	Exchangeable bases (cmol <sub>c</sub> kg <sup>-1</sup> )	Exchangeable bases (cmol <sub>c</sub> kg <sup>-1</sup> )	SEB <sup>1</sup>	CEC	BS <sup>2</sup>	CaCl <sub>2</sub> - Si
Nitisol	5.8	4.8	4.3	1.9	1.8	0.1	8.1	25.8	31	16.8 (0.8)b
Andosol	5.8	4.8	2.1	2.1	1.3	0.2	5.7	47.6	12	31.3 (1.6)b
Vertisol	7.2	5.9	42.1	7.9	0.4	0.8	51.2	59.9	86	55.1 (11.0)a

(a)

<sup>1</sup> Sum of exchangeable bases

<sup>2</sup> BS=SEB/CEC\*100

Soil	Total elemental concentration (cmol <sub>c</sub> kg <sup>-1</sup> )		Total elemental concentration (cmol <sub>c</sub> kg <sup>-1</sup> )		Total elemental concen
	Ca		Mg		K
Nitisol	11.5		15.6		6.2
Andosol	15.8		83.6		5.0
Vertisol	56.6		49.6		4.2

(b)

<sup>3</sup> TRB is the sum of the total contents of major alkaline and alkaline-earth cations (Herbillon 1986)

<sup>4</sup> The non-exchangeable cation content is the difference between the total and exchangeable content for each cation.

<sup>5</sup> Sum of the contents of non-exchangeable bases (TRB – SEB).

**Table 3 :** Mineral contents and balances in sugarcane leaves: average (n=3) values of foliar contents of Si, Ca, Mg, K; sum of cations Ca, Mg, K (Sc), cationic proportions in Sc, and Mg/Ca atomic ratio. SE are given under brackets for the leaf mineral contents.

	Leaf mineral content (g kg <sup>-1</sup> )	Leaf mineral content (g kg <sup>-1</sup> )	Leaf mineral content (g kg <sup>-1</sup> )	Leaf mineral content (g kg <sup>-1</sup> )	Sc	Cationic proportion in Sc (%)	Cationic proportion in Sc (%)	Cationic proportion in Sc (%)	Ra Mg
Site	Si	Ca	Mg	K	cmol <sub>c</sub> kg <sup>-1</sup>	Ca	Mg	K	
Nitisol	7.0 (0.3)c	2.6 (0.1)b	1.2 (0.0)b	13.2 (0.1)a	56	23	17	60	0.7
Andosol	14.7 (0.2)b	2.1 (0.1)b	2.2 (0.1)a	11.8 (0.4)b	59	18	31	51	1.7
Vertisol	21.0 (1.1)a	7.0 (0.3)a	1.5 (0.2)b	12.5 (0.3)ab	79	44	15	40	0.3

**Table 4 :** Average values (n=3, SE into brackets) of ash, carbon, cellulose, hemicellulose and lignin concentrations of the sugarcane leaf samples, expressed as dry weight percentages (g kg<sup>-1</sup>DW) and/or ash-free dry weight percentages (g kg<sup>-1</sup>AFDW).

Site name	Ash	Carbon	Carbon	Cellulose	Cellulose	Hemicellulose	Hemicellulose	Lignin	Lig
	DW	DW	AFDW	DW	AFDW	DW	AFDW	DW	AF
Nitisol	54 (1)c	469 (1)a	496 (1)c	354 (4)a	374 (4)a	322 (5)ab	341 (5)b	53 (1)a	56
Andosol	66 (1)b	465 (1)a	498 (1)b	341 (1)b	365 (1)b	337 (0)a	360 (0.7)a	40 (1)c	43
Vertisol	89 (3)a	455 (2)b	500 (1)a	324 (2)c	356 (0.1)c	312 (7)b	343 (0.7)b	46 (2)b	50

## References

- Abou-El-Enin O.H., Fadel J.G. & MacKill D.J. (1999) Differences in chemical composition and fibre digestion of rice straw with, and without, anhydrous ammonia from 53 rice varieties. *Animal Feed Science and Technology* **79** , 129–136.
- Adrees M., Ali S., Rizwan M., Zia-ur-rehman M., Ibrahim M., Abbas F., ... Kashif M. (2015) Ecotoxicology and Environmental Safety Mechanisms of silicon-mediated alleviation of heavy metal toxicity in plants : A review. *Ecotoxicology and Environmental Safety* **119** , 186–197.
- Agbagla-Dohnani A., Nozière P., Clément G. & Doreau M. (2001) In sacco degradability, chemical and morphological composition of 15 varieties of European rice straw. *Animal Feed Science and Technology* **94** , 15–27.
- Alabouvette C. (1999) Fusarium wilt suppressive soils: an example of disease-suppressive soils. *Australasian Plant Pathology* **28** , 57–64.
- Alabouvette C., Olivain C. & Steinberg C. (2006) Biological control of plant diseases: the European situation. *European Journal of Plant Pathology* **114** , 329–341.
- Alexandre A., Webb E., Landais A., Piel C., Devidal S., Sonzogni C., ... Roy J. (2019) Effects of grass leaf anatomy, development and light/dark alternation on the triple oxygen isotope signature of leaf water and phytoliths: insights for a new proxy of continental atmospheric humidity. *Biogeosciences Discussions* **16** , 4613–4625.
- Ando H., Kakuda K.I., Fujii H., Suzuki K. & Ajiki T. (2002) Growth and canopy structure of rice plants grown under field conditions as affected by si application. *Soil Science and Plant Nutrition* **48** , 429–432.
- Bauer P., Elbaum R. & Weiss I.M. (2011) Calcium and silicon mineralization in land plants: Transport, structure and function. *Plant Science* **180** , 746–756.
- Bonilla P.-S. (2001) Variation in the cellulose, lignin and silica contents of various parts of difference rice (*Oryza sativa* L.) cultivars. *The Philippine agricultural scientist* **84** , 126–137.
- Boudon G., Dagain J., Semet M.P. & Westercamp D. (1987) Carte géologique 1: 20 000 du massif volcanique de la Soufrière (Département de la Guadeloupe, Petites Antilles). *BRGM, Paris* .
- Cai K., Gao D., Luo S., Zeng R., Yang J. & Zhu X. (2008) Physiological and cytological mechanisms of silicon-induced resistance in rice against blast disease. *Physiologia Plantarum* **134** , 324–333.
- Camargo M.S. de, Amorim L. & Gomes Junior A.R. (2013) Silicon fertilisation decreases brown rust incidence in sugarcane. *Crop Protection* **53** , 72–79.
- Chadwick O.A., Gavenda R.T., Kelly E.F., Ziegler K., Olson C.G., Crawford Elliott W. & Hendricks D.M. (2003) The impact of climate on the biogeochemical functioning of volcanic soils. *Chemical Geology* **202** , 195–223.
- Chao T.T. & Sanzolone R.F. (1992) Decomposition techniques. *Journal of Geochemical Exploration* **44** , 65–106.

- Churchman G.J. & Lowe D.. (2012) Alteration, formation, and occurrence of minerals in soils. *Handbook of Soil Sciences: Properties and Processes* **1** , 20–72.
- Colmet-Daage F. & Lagache P. (1965) Caractéristiques de quelques groupes de sols dérivés de roches volcaniques aux antilles françaises. *Cahiers ORSTOM. Série Pédologie* **3** , 91–121.
- Cooke J., DeGabriel J.L. & Hartley S.E. (2016) The functional ecology of plant silicon: geoscience to genes. *Functional Ecology* **30** , 1270–1276.
- Cooke J. & Leishman M.R. (2012) Tradeoffs between foliar silicon and carbon-based defences: Evidence from vegetation communities of contrasting soil types. *Oikos* **121** , 2052–2060.
- Cooke J. & Leishman M.R. (2016) Consistent alleviation of abiotic stress with silicon addition: a meta-analysis. *Functional Ecology* **30** , 1340–1357.
- Corbineau R., Reyerson P.E., Alexandre A. & Santos G.M. (2013) Towards producing pure phytolith concentrates from plants that are suitable for carbon isotopic analysis. *Review of Palaeobotany and Palynology* **197** , 179–185.
- Cornelis J.-T. & Delvaux B. (2016) Soil processes drive the biological silicon feedback loop. *Functional Ecology* **30** , 1298–1310.
- Coskun D., Deshmukh R., Sonah H., Menzies J.G., Reynolds O., Ma J.F., ... Bélanger R.R. (2019) The controversies of silicon's role in plant biology. *New Phytologist* **221** , 67–85.
- Deshmukh R. & Bélanger R.R. (2016) Molecular evolution of aquaporins and silicon influx in plants. *Functional Ecology* **30** , 1277–1285.
- Epstein E. (1994) The anomaly of silicon in plant biology. *Proceedings of the National Academy of Sciences of the United States of America* **91** , 11–17.
- Epstein E. (1999) Silicon. *Annu. Rev. Plant Physiol. Plant Mol. Biol.* **50** , 641–664.
- Epstein E. (2009) Silicon: Its manifold roles in plants. *Annals of Applied Biology* **155** , 155–160.
- Euliss K.W., Dorsey B.L., Benke K.C., Banks M.K. & Schwab A.P. (2005) The use of plant tissue silica content for estimating transpiration. *Ecological Engineering* **25** , 343–348.
- Exley C. (2015) A possible mechanism of biological silicification in plants. *Frontiers in Plant Science* **6** , 1–7.
- Fauteux F., Chain F., Belzile F., Menzies J.G. & Bélanger R.R. (2006) The protective role of Si in the Arabidopsis-powdery mildew pathosystem. *Proceedings of the National Academy of Sciences* **103** , 17554–17559.
- Fauteux F., Rémus-Borel W., Menzies J.G. & Bélanger R.R. (2005) Silicon and plant disease resistance against pathogenic fungi. *FEMS Microbiology Letters* **249** , 1–6.
- Fraysse F., Pokrovsky O.S., Schott J. & Meunier J.D. (2009) Surface chemistry and reactivity of plant phytoliths in aqueous solutions. *Chemical Geology* **258** , 197–206.
- Frew A., Powell J.R., Sallam N., Allsopp P.G. & Johnson S.N. (2016) Trade-Offs between Silicon and Phenolic Defenses may Explain Enhanced Performance of Root Herbivores on Phenolic-Rich Plants. *Journal of Chemical Ecology* **42** , 768–771.
- Godin B., Agneessens R., Gerin P. & Delcarte J. (2014) Structural carbohydrates in plant biomasses: correlations between the detergent fiber and the dietary fiber methods. *Journal of Agricultural and Food Chemistry* **62** , 5609–5616.
- Godin B., Agneessens R., Gerin P. & Delcarte J. (2015) Lignin in plant biomasses: comparative metrological assessment of the detergent fiber and the insoluble dietary fiber methods. *Cellulose* **22** , 2235–2340.



- Godin B., Agneessens R., Gofflot S., Lamaudière S., Sinnaeve G., Gerin P.A. & Delcarte J. (2011) T0792.- Revue biblio sur méthodes analyse des poysacch structuraux des biomasses lignocellulosiques. *Biotechnologie, Agronomie, Société et Environnement* **15** , 165–182.
- Guerriero G., Hausman J.-F. & Legay S. (2016) Silicon and the Plant Extracellular Matrix. *Frontiers in Plant Science* **7** , 1–8.
- Guerriero G., Law C., Stokes I., Moore K.L. & Exley C. (2018) Rough and tough. How does silicic acid protect horsetail from fungal infection? *Journal of Trace Elements in Medicine and Biology* **47** , 45–52.
- Hartley S.E., Fitt R.N., McLarnon E.L. & Wade R.N. (2015) Defending the leaf surface: intra- and inter-specific differences in silicon deposition in grasses in response to damage and silicon supply. *Frontiers in Plant Science* **6** , 35.
- Hasan S., Shimojo M. & Goto I. (1993) Chemical components influencing lodging resistance of rice plant and its straw digestibility in vitro. *Asian Australas. J. Anim. Sci* **6** , 41–44.
- Haymsom M. & Chapman L. (1975) Some aspects of the calcium silicate trials at Mackay. *Proceedings of the Queensland Society of Sugar Cane Technologists*. **42** , 117–122.
- Henriet C., Bodarwé L., Dorel M., Draye X. & Delvaux B. (2008a) Leaf silicon content in banana (*Musa* spp.) reveals the weathering stage of volcanic ash soils in Guadeloupe. *Plant and Soil* **313** , 71–82.
- Henriet C., Draye X., Oppitz I., Swennen R. & Delvaux B. (2006) Effects, distribution and uptake of silicon in banana (*Musa* spp.) under controlled conditions. *Plant and Soil* **287** , 359–374.
- Henriet C., De Jaeger N., Dorel M., Opfergelt S. & Delvaux B. (2008b) The reserve of weatherable primary silicates impacts the accumulation of biogenic silicon in volcanic ash soils. *Biogeochemistry* **90** , 209–223.
- Herbillon A. (1986) Chemical estimation of weatherable minerals present in the diagnostic horizon of low activity clay soils. *Proceedings of the 8th International Classification Work- shop: Classification, Characterization, and Utilization of Ultisols. Part I. EMBRAPA, Rio de Janeiro*, 39–48.
- Hodson M.J. (2019) The relative importance of cell wall and lumen phytoliths in carbon sequestration in soil: A hypothesis. *Frontiers in Earth Science* **7** , 167.
- Hodson M.J., Sangster A.G. & Parry D.W. (1985) An ultrastructural study on the developmental phases and silicification of the glumes of *Phalaris canariensis* L. *Annals of Botany* **55** , 649–665.
- Hodson M.J., White P.J., Mead A. & Broadley M.R. (2005) Phylogenetic variation in the silicon composition of plants. *Annals of Botany* **96** , 1027–1046.
- Issaharou-Matchi I., Barboni D., Meunier J.D., Saadou M., Dussouillez P., Contoux C. & Zirihi-Guede N. (2016) Intraspecific biogenic silica variations in the grass species *Pennisetum pedicellatum* along an evapotranspiration gradient in South Niger. *Flora: Morphology, Distribution, Functional Ecology of Plants* **220** , 84–93.
- IUSS (2014) World reference base for soil classification 2014. *Food and Agriculture Organisation of the United Nations, Rome* .
- Jones L.H.P. & Handreck K.A. (1967) Silica In Soils, Plants, and Animals. *Advances in Agronomy* **19** , 107–149.
- Kang J., Zhao W. & Zhu X. (2016) Silicon improves photosynthesis and strengthens enzyme activities in the C3 succulent xerophyte *Zygophyllum xanthoxylum* under drought stress. *Journal of Plant Physiology* **199** , 76–86.
- Katz O. (2019) Silicon content is a plant functional trait: implications in a changing world. *Flora* **254** , 88–94.

- Kaufman P.B., Dayanandan P. & Franklin C.I. (1985) Structure and function of silica bodies in the epidermal system of grass shoots. *Annals of Botany* **55** , 487–507.
- Keeping M.G., Kvedaras O.L. & Bruton A.G. (2009) Epidermal silicon in sugarcane: Cultivar differences and role in resistance to sugarcane borer *Eldana saccharina*. *Environmental and Experimental Botany* **66** , 54–60.
- Keeping M.G. & Meyer J.H. (2006) Silicon-mediated resistance of sugarcane to *Eldana saccharina* Walker (Lepidoptera: Pyralidae): Effects of silicon source and cultivar. *Journal of Applied Entomology* **130** , 410–420.
- Keeping M.G., Meyer J.H. & Sewpersad C. (2013) Soil silicon amendments increase resistance of sugarcane to stalk borer *Eldana saccharina* Walker (Lepidoptera: Pyralidae) under field conditions. *Plant and Soil* **363** , 297–318.
- Kelly E.F. (1990) Methods for extracting opal phytoliths from soil and plant material. In *Workshop on biotic indicators of global change, Seattle, Washington*.
- Kido N., Yokoyama R., Yamamoto T., Furukawa J., Iwai H., Satoh S. & Nishitani K. (2015) The matrix polysaccharide (1;3,1;4)-2- d -glucan is involved in silicon-dependent strengthening of rice cell wall. *Plant and Cell Physiology* **56** , 268–276.
- Kitajima K., Llorens A.-M., Stefanescu C., Timchenko M.-V., Lucas P.-W. & Wright S.-J. (2012) How cellulose-based leaf toughness and lamina density contribute to long leaf lifespans of shade-tolerant species. *New Phytologist* **195** , 640–652.
- Kitajima K., Wright S.J. & Westbrook J.W. (2016) Leaf cellulose density as the key determinant of inter- and intra-specific variation in leaf fracture toughness in a species-rich tropical forest. *Interface Focus* **6** , 20150100.
- Klotzbücher T., Klotzbücher A., Kaiser K., Vetterlein D., Jahn R. & Mikutta R. (2018) Variable silicon accumulation in plants affects terrestrial carbon cycling by controlling lignin synthesis. *Global Change Biology* **24** , 183–189.
- Klotzbücher T., Marxen A., Vetterlein D., Schneiker J., Türke M., van Sinh N., ... Jahn R. (2015) Plant-available silicon in paddy soils as a key factor for sustainable rice production in Southeast Asia. *Basic and Applied Ecology* **16** , 665–673.
- Komorowski J.-C., Boudon G., Semet M., Beauducel F., Anténor-Habazac C., Bazin S. & Hammouya G. (2005) Guadeloupe. In *Volcanic Hazard Atlas of The Lesser Antilles* . pp. 65–102. Seismic Research Unit, Univesrity of the West Indies.
- Kumar S. & Elbaum R. (2018) Interplay between silica deposition and viability during the life span of sorghum silica cells. *New Phytologist* **217** , 1137–1145.
- Kumar S., Milstein Y., Brami Y., Elbaum M. & Elbaum R. (2017a) Mechanism of silica deposition in sorghum silica cells. *New Phytologist* **213** , 791–798.
- Kumar S., Soukup M. & Elbaum R. (2017b) Silicification in grasses: variation between different cell types. *Frontiers in plant science* **8** , 438.
- Law C. & Exley C. (2011) New insight into silica deposition in horsetail (*Equisetum arvense*). *BMC Plant Biology* **11** , 112.
- Leroy N., de Tombeur F., Walgraffe Y., Cornélis J.-T. & Verheggen F. (2019) Silicon and Plant Natural Defenses against Insect Pests : Impact on Plant Volatile Organic Compounds and Cascade Effects on Multitrophic Interactions. *Plants* **8** , 444.
- Li F., Zhang M., Guo K., Hu Z., Zhang R., Feng Y., ... Peng L. (2015) High-level hemicellulosic arabinose predominately affects lignocellulose crystallinity for genetically enhancing both plant lodging resistance and

biomass enzymatic digestibility in rice mutants. *Plant Biotechnology Journal* **13** , 514–525.

Lucas Y., Luizao F.J., Chauvel A., Rouiller J. & Nahon D. (1993) The relation between biological activity of the rain forest and mineral composition of soils. *Science* **260** , 521–523.

Ma J.F., Tamai K., Yamaji N., Mitani N., Konishi S., Katsuhara M., ... Yano M. (2006) A silicon transporter in rice. *Nature* **440** , 688–691.

Massey F.P. & Hartley S.E. (2006) Experimental demonstration of the antiherbivore effects of silica in grasses: impacts on foliage digestibility and vole growth rates. *Proceedings of the Royal Society B: Biological Sciences* **273** , 2299–2304.

McCray J.M., Rice R.W. & Ezenwa I. V. Sugarcane Leaf Tissue Sample Preparation for Diagnostic Analysis. *IFAS Extension* , 1–4.

McNaughton S.J., Tarrant J.L., McNaughton M.M. & Davis R.D. (1985) Silica as a Defense against Herbivory and a Growth Promotor in African Grasses. *Ecology* **66** , 528–535.

Meunier J.D., Barboni D., Anwar-ul-Haq M., Levard C., Chaurand P., Vidal V., ... Keller C. (2017) Effect of phytoliths for mitigating water stress in durum wheat. *New Phytologist* **215** , 229–239.

Meunier J.D., Colin F. & Alarcon C. (1999) Biogenic silica storage in soils. *Geology* **27** , 835–838.

Motomura H., Fujii T. & Suzuki M. (2004) Silica Deposition in Relation to Ageing of Leaf Tissues in *Sasa veitchii* A re ) Rehder ( Poaceae : Bambusoideae ). *Annals of Botany* **93** , 235–248.

Motomura H., Fujii T. & Suzuki M. (2006) Silica Deposition in Abaxial Epidermis before the Opening of Leaf Blades of *Pleioblastus chino* ( Poaceae , Bambusoideae ). *Annals of Applied Biology* **97** , 513–519.

Nakamura R., Cornelis J.-T., de Tombeur F., Nakagawa M. & Kitajima K. (2020) Comparative analysis of borate fusion versus sodium carbonate extraction for quantification of silicon contents in plants. *Journal of Plant Research* **133** , 271–277.

Ndayiragije S. & Delvaux B. (2003) Coexistence of allophane, gibbsite, kaolinite and hydroxy-Al-interlayered 2:1 clay minerals in a perudic Andosol. *Geoderma* **117** , 203–214.

Neu S., Schaller J. & Dudel E.G. (2017) Silicon availability modifies nutrient use efficiency and content, C:N:P stoichiometry, and productivity of winter wheat (*Triticum aestivum* L.). *Scientific Reports* **7** , 40829.

Olsen S.R., Sommers L.E. & Page A.L. (1982) Methods of soil analysis. Part 2. Chem. Microbiol. Prop. Phosphorus. *American Society of Agronomy, Inc. Soil Science Society of America, Inc.* **9** , 403–430.

Perry C.C. & Fraser M.A. (1991) Silica deposition and ultrastructure in the cell wall of *Equisetum arvense*: The importance of cell wall structures and flow control in biosilicification? *Philosophical Transactions of the Royal Society B: Biological Sciences* **334** , 149–157.

Perry C.C. & Keeling-Tucker T. (2000) Biosilicification: The role of the organic matrix in structure control. *Journal of Biological Inorganic Chemistry* **5** , 537–550.

Quigley K.M. & Anderson T.M. (2014) Leaf silica concentration in Serengeti grasses increases with watering but not clipping: insight from a common garden study and literature review. *Frontiers in Plant Science* **5** , 568.

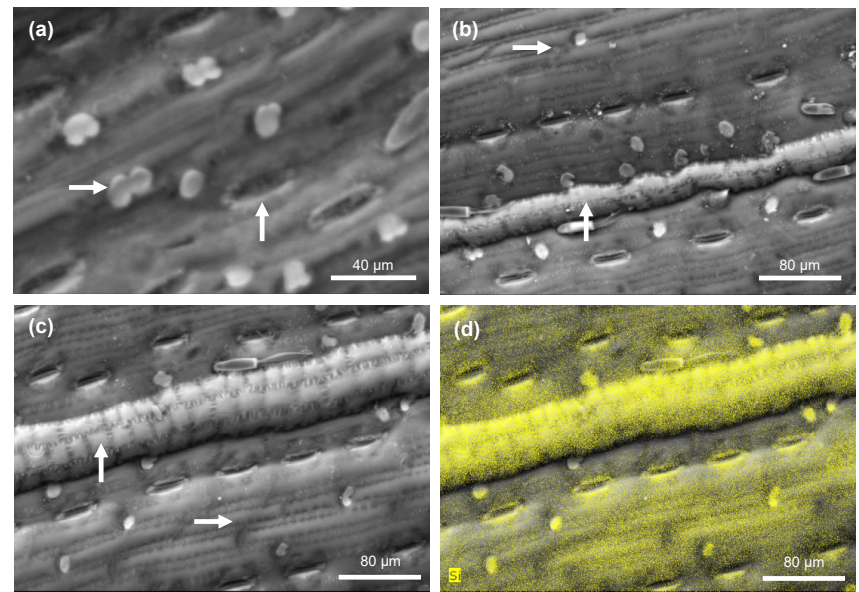
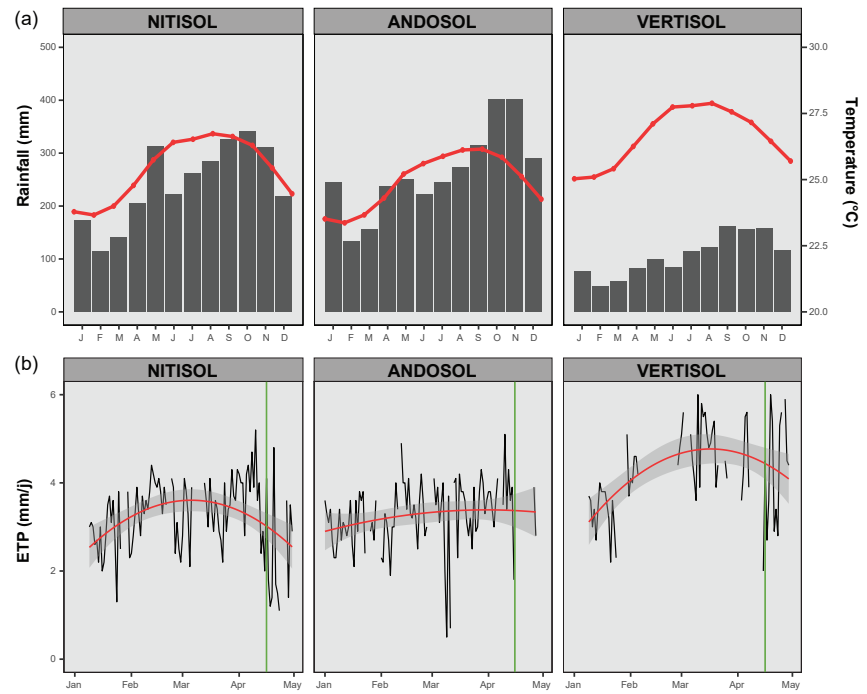
Quigley K.M., Donati G.L. & Anderson T.M. (2016) Variation in the soil “silicon landscape” explains plant silica accumulation across environmental gradients in Serengeti. *Plant and Soil* **410** , 217–229.

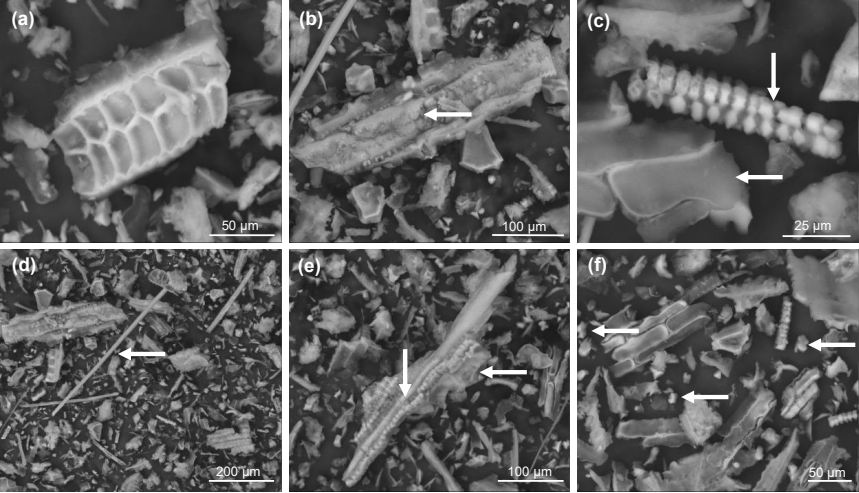
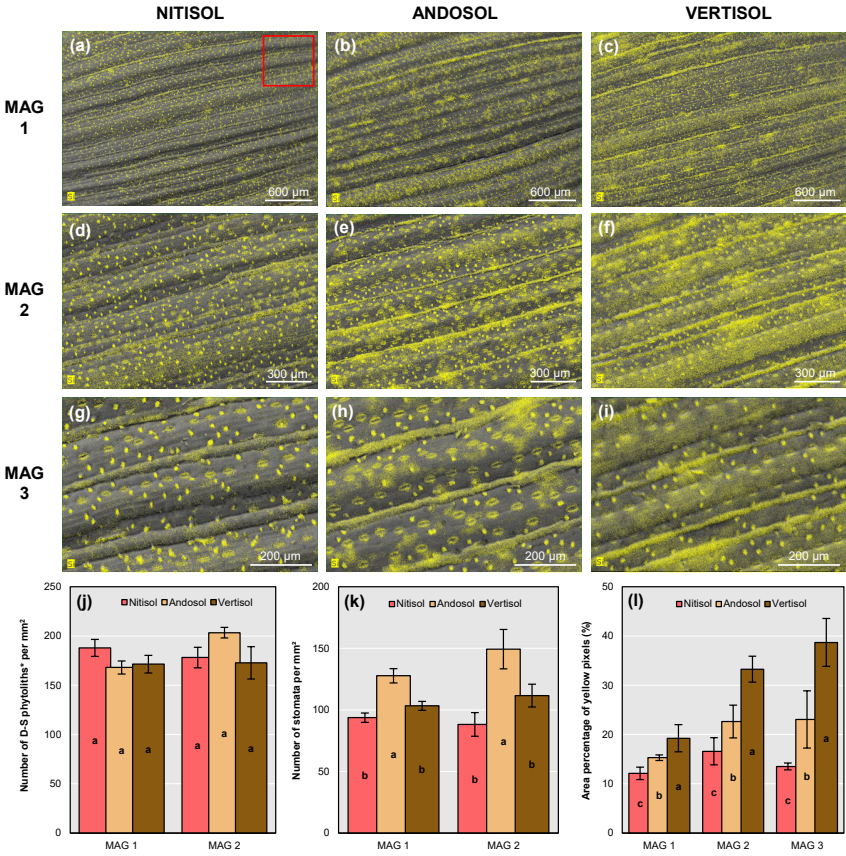
Rai D. & Kittrick J.A. (1989) Mineral equilibria and the soil system. In *Minerals in Soil Environments* . (ed S.S.S. of America), pp. 161–198. Madison, USA.

Raven J.A. (1983) The transport and function of silicon in plants. *Biological Reviews* **58** , 179–207.

- Rosen A.M. & Weiner S. (1994) Identifying ancient irrigation: a new method using opaline phytoliths from emmer wheat. *Journal of Archaeological Science* **21** , 125–132.
- Sangster A.G., Hodson M.J. & Tubb H.J. (2001) Silicon deposition in higher plants. In *Silicon in Agriculture* , Elsevier. pp. 85–113. The Netherlands.
- Sauer D., Saccone L., Conley D.J., Herrmann L. & Sommer M. (2006) Review of methodologies for extracting plant-available and amorphous Si from soils and aquatic sediments. *Biogeochemistry* **80** , 89–108.
- Schaller J., Brackhage C. & Dudel E.G. (2012) Silicon availability changes structural carbon ratio and phenol content of grasses. *Environmental and Experimental Botany* **77** , 283–287.
- Schaller J., Heimes R., Ma J.F., Meunier J.-D., Shao J.F., Fujii-Kashino M. & Knorr K.H. (2019) Silicon accumulation in rice plant aboveground biomass affects leaf carbon quality. *Plant and Soil* **444** , 399–407.
- Schoelynck J., Bal K., Backx H., Okruszko T., Meire P. & Struyf E. (2010) Silica uptake in aquatic and wetland macrophytes: A strategic choice between silica, lignin and cellulose? *New Phytologist* **186** , 385–391.
- Schoelynck J. & Struyf E. (2016) Silicon in aquatic vegetation. *Functional Ecology* **30** , 1323–1330.
- Shen H.S., Ni D. & Sundstol F. (1998) Studies on untreated and urea-treated rice straw from three cultivation seasons: 1. Physical and chemical measurements in straw and straw fractions. *Animal Feed Science and Technology* **73** , 243–261.
- Simpson K.J., Wade R.N., Rees M., Osborne C.P. & Hartley S.E. (2017) Still armed after domestication? Impacts of domestication and agronomic selection on silicon defences in cereals. *Functional Ecology* **31** , 2108–2117.
- Van Soest P.J. (1973) Collaborative study of acid-detergent fiber and lignin. *Journal of the AOAC* **56** , 781–784.
- Van Soest P.J. & Wine R. (1967) Use of detergents in the analysis of fibrous feeds. IV. Determination of plant cell wall constituents. *Journal of the AOAC* **50** , 50–55.
- Soukup M., Martinka M., Bosnić D., Čaplovičová M., Elbaum R. & Lux A. (2017) Formation of silica aggregates in sorghum root endodermis is predetermined by cell wall architecture and development. *Annals of Botany* **120** , 739–753.
- Stotzky G. (1986) Influence of soil minerals colloids on metabolic processes, growth, adhesion, and ecology of microbes and viruses. In *Interactions of soil minerals with natural organisms and microbes*. (eds P.M. Huang & M. Schnitzer), pp. 305–428. Madison, Wisconsin.
- Stotzky G. & Martin T. (1963) Soil mineralogy in relation to the spread of Fusarium wilt of banana in Central America. *Plant and Soil* **18** , 317–337.
- Suzuki S., Ma J.F., Yamamoto N., Hattori T., Sakamoto M. & Umezawa T. (2012) Silicon deficiency promotes lignin accumulation in rice. *Plant Biotechnology* **29** , 391–394.
- de Tombeur F., Turner B.L., Laliberté E., Lambers H. & Cornelis J.-T. (2020) Silicon dynamics during 2 million years of soil development in a coastal dune chronosequence under a Mediterranean climate. *Ecosystems* .
- Tubana B.S., Babu T. & Datnoff L.E. (2016) A Review of Silicon in Soils and Plants and Its Role in US Agriculture. *Soil Science* **181** , 1.
- USDA's Soil Survey Laboratory Staff (2017) *Soil survey manual. USDA Handbook 18. Government Printing Office, Washington, D. C.* , USDA Handb. (ed G.P. Office), Washington, D. C.
- Yamamoto T., Nakamura A., Iwai H., Ishii T., Ma J.F., Yokoyama R., ... Furukawa J. (2012) Effect of silicon deficiency on secondary cell wall synthesis in rice leaf. *Journal of Plant Research* **125** , 771–779.

Yoshida S., Onishi Y. & Kitagishi K. (1959) The chemical nature of silicon in rice plant. *Soil Science and Plant Nutrition* **5**, 23–27.



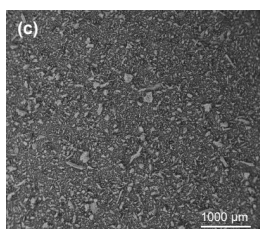
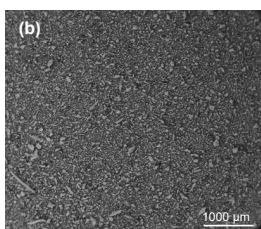
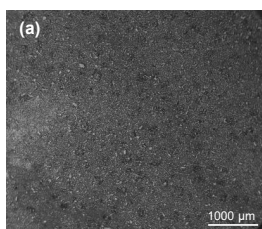


NITISOL

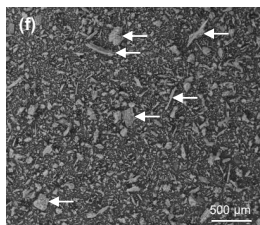
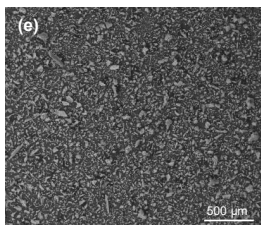
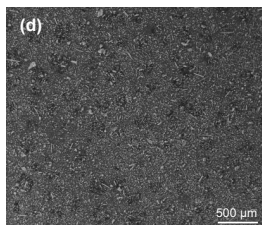
ANDOSOL

VERTISOL

MAG  
1



MAG  
2



MAG  
3

